# A Numerical method for steady linear waves due to a two-dimensional shallowly submerged hydrofoil

B. de'Vidovich, G. Trincas
*Department of Naval Architecture, University of Trieste, Italy*

## Abstract

A design tool for predicting the flow past submerged hydrofoils is described, intended to give the designer guidelines in estimating efficiency of alternative hydrofoil configurations in motion at arbitrary Froude number below the free surface. A complete set of hydrodynamic characteristics may be evaluated, stored and represented by simple and exhaustive diagrams for each hydrofoil. The flow is simulated numerically by a finite number of singularities positioned along the foil's camber line. The exact free-surface boundary condition is replaced by a linearized condition since eventual inaccuracies in results may be not so relevant in many engineering applications. Numerical results of the performance characteristics are given for a NACA 16-012 symmetrical wing section which is particularly suitable for high-speed hydrofoil applications because of its low cavitation number.

## 1 Introduction

In recent years there has been a growing demand for new high–speed vehicles with shallowly submerged hydrofoils to reduce the hull resistance. To evaluate potential efficiency and optimise the performance characteristics of innovative engineering solutions, the simple and efficient numerical code presented in this paper can be very useful at very early design stages. It is intended to help the designer to estimate feasibility and efficiency of alternative hydrofoils at different submergences and angles of incidence, and to select the optimal geometry configuration on the basis of the achievable drag reduction and lift improvement, leading to lower fuel consumption and smaller horsepower per unit speed.

It is the purpose of this paper to find out through numerical computation how the lift and drag are influenced by the free–surface waves which are affected greatly by the submerged depth and angle of incidence. A linear formulation of the hydrofoil problem has been adopted which could be easily extended to the study of arbitrary two–dimensional lifting surfaces. In an effort to improve an earlier work [1], investigation is carried out to ascertain from an engineering viewpoint what shallow submergence does mean or, in other terms, to shed light into the range of significant parameters for which linearization

of the free surface is still valid. In practical terms, the proper application of the linearized wave theory in estimating flow characteristics of a two–dimensional shallowly submerged hydrofoil gives an opportunity to improve the design quality and cut the design time, partially eliminating the need for costly model experiments.

# 2 Formulation of the problem

Even if there have been several studies on lift and distribution of the pressure acting on the surface of hydrofoils starting from the fundamental work carried out by Kočin [3], as well as on the effect of a near free surface on hydrofoil performance, the mathematical formulation is here summarized and enhanced for the treatment of the steady noncavitating potential flow of a uniform stream past a shallowly submerged hydrofoil with infinite span under linearization of the free–surface boundary condition. The approach is based upon the use of singularity distribution and reduction of governing integral equation to a set of linear algebraic equations. The most important and ultimate objective is to find out how the two–dimensional hydrodynamic characteristics of a hydrofoil are affected by the influence of the surface wave motion created.

## 2.1 Exact free surface condition

When surface tension is neglected and breaking waves are not considered, the free–surface boundary condition can be expressed mathematically by two nonlinear equations, representings the kinematic and the dynamic condition.

Designate the free–surface elevation by $\zeta = \zeta(x, y; t)$, where $x$- and $y$–axes are taken on the undisturbed free surface and $z$–axis is oriented vertically upwards. The so–called kinematic boundary condition that supposes the fluid particles remaining on the free surface during the deformation, can be satisfied by

$$\zeta(x_o + udt, y_o + vdt, t_o + dt) = z_o + wdt \tag{1}$$

or, in other terms

$$u\frac{\partial \zeta}{\partial x} + v\frac{\partial \zeta}{\partial y} + \frac{\partial \zeta}{\partial t} = w \tag{2}$$

where $u$, $v$ and $w$ are the steady–state velocity components.

The condition of pressure being uniform on the free surface combined with Bernoulli's equation, leads to the free surface dynamic condition

$$\zeta = \frac{1}{2g}\left(V_o^2 - u^2 - v^2 - w^2\right) \tag{3}$$

in which $V_o$ denotes the undisturbed flow velocity.

## 2.2 Linearization by a perturbation method

Equations (2) and (3) are the free–surface boundary condition in a very general formulation. If weak interaction between the body and the free surface is assumed, the wave elevations should be relatively small with low fluid velocity gradients. Hence, the exact free–surface boundary condition may be linearized by a perturbative approach. An appropriate perturbation parameter $\varepsilon$ is introduced, which can be considered representative of the wave disturbance superimposed, as a small deviation, upon the undisturbed flow. In the case of a hydrofoil, the body is initially a flat horizontal plane and the flow remains undisturbed ($\varepsilon = 0$). When $\varepsilon$ increases, the foil takes its own geometrical

characteristics and the flow adapts itself. If the hydrofoil were without any camber and angle of incidence, the thickness–to–chord ratio could be assumed as $\varepsilon$ parameter. But if one wants to model the flow past a hydrofoil properly, also the angle of incidence and the camber have to be proportional to $\varepsilon$, so that they are zero when $\varepsilon = 0$. Under these assumptions, the flow characteristics $(\varphi, \psi, u, v, \zeta, \ldots)$ may be expressed in power series of $\varepsilon$. For example, the the $x$–component of the velocity may be written as

$$u = u_o + u_1\varepsilon + u_2\varepsilon^2 + \ldots \tag{4}$$

where $u_o$ is the $x$–component of the undisturbed flow.

Since it is very difficult to apply the exact boundary condition on the free surface, one can calculate the value of the flow characteristics there by a Taylor series expansion. In this way, one obtains

$$u(x,y,\zeta) = u(x,y,0) + \left(\frac{\partial u}{\partial z}\right)_{x,y,0}\zeta + \frac{1}{2}\left(\frac{\partial^2 u}{\partial z^2}\right)_{x,y,0}\zeta^2 + \frac{1}{6}\left(\frac{\partial^3 u}{\partial z^3}\right)_{x,y,0}\zeta^3 + \ldots \tag{5}$$

Equations (4) and (5) can then be combined to obtain a double power series in terms of $\varepsilon$ and $\zeta$. Since the free–surface elevation $\zeta$ can be expressed by a power series of $\varepsilon$ (4), one can obtain a single power series of $\varepsilon$. Finally, the $x$–component of the velocity on the free surface has the expansion

$$\begin{aligned} u(x,y,\zeta) \;=\; & (u_o + u_1\varepsilon + u_2\varepsilon^2 + \ldots) + \\ & \left(\frac{\partial u_o}{\partial z} + \frac{\partial u_1}{\partial z}\varepsilon + \frac{\partial u_2}{\partial z}\varepsilon^2 + \ldots\right)\cdot(\zeta_o + \zeta_1\varepsilon + \zeta_2\varepsilon^2 + \ldots) + \\ & \frac{1}{2}\left(\frac{\partial^2 u_o}{\partial z^2} + \frac{\partial^2 u_1}{\partial z^2}\varepsilon + \frac{\partial^2 u_2}{\partial z^2}\varepsilon^2 + \ldots\right)\cdot(\zeta_o + \zeta_1\varepsilon + \zeta_2\varepsilon^2 + \ldots)^2 + \ldots \end{aligned} \tag{6}$$

where all terms in the right side of equation (6) are calculated at point $(x, y, 0)$.

Expressions (6) are then inserted into equations (2) and (3), retaining only the first–order terms of $\varepsilon$. If one assumes that the flow is steady and the direction of undisturbed velocity is against $x$–axis, after algebraic manipulation the linearized free–surface boundary condition may be given in the form

$$\frac{\partial u_1}{\partial x} + \nu w_1 = 0 \qquad ; \quad \zeta = \frac{V_o}{g}u_1 \tag{7}$$

where $u_1$ and $w_1$ are the first–order velocity components, $\nu = g/V_o^2$ is the fundamental wave number, and $g$ is the acceleration of gravity.

## 2.3 Field equations

Expression for singularities near the free surface has now to be determined by applying, beyond the linearized free surface condition, the radiation condition and the motion–damping condition at infinite depth. For sake of brevity, the mathematical treatment is not illustrated. Only the final formulation is given and discussed.

Flow characteristics $(\varphi, \psi, u, v)$ are decomposed as the sum of four terms:

1. The first term is the basis characteristic of the singularity; for instance, the potential $\varphi_S$.
2. The second term, $\varphi_C$, is due to its gravity image, e.g., it is a singularity equal to the previous one, but positioned simmetrically with respect to the undisturbed free surface.
3. The third term, $\varphi_L$, derives from the application of the free–surface condition. It is expressed through an inverse Fourier transform and cannot be reduced to a simple algebraic form.

4. The fourth term, $\varphi_0$, is introduced to comply with the radiation condition.

Previous treatment is general and valid also for three-dimensional situations. In the case of two-dimensional flow, the term arising from application of the radiation condition requires no wave behind the body. If one considers the flow behaviour far away from the singularity, the $(S)$ and $(C)$ terms numerically decay, while the $(L)$ and $(O)$ terms compensate each other far upstream because of the radiation condition and are summed downstream where they have the same values at every point. To determine the wave elevation after singularity, it is then sufficient to double the amplitude derived from the term $(O)$ which can be immediately calculated without evaluating the term $(L)$ which is quite complicated and expensive from a computational point of view.

As an example, the total vortex potential is represented as

$$\begin{aligned}
\varphi &= \frac{\Gamma}{2\pi}(\varphi_S + \varphi_C + \varphi_L + \varphi_0) \qquad ; \quad \nu = \frac{g}{V_o^2} \\
\varphi_S &= \arctan\left(\frac{y-y_o}{x-x_o}\right) \qquad ; \quad \varphi_C = -\arctan\left(\frac{y+y_o}{x-x_o}\right) \qquad (8) \\
\varphi_L &= 2\int_o^\infty \frac{e^{\lambda\frac{x+y_o}{-y_o}}}{\lambda+\nu y_o}\sin\left(\lambda\frac{x-x_o}{-y_o}\right)d\lambda \quad ; \quad \varphi_0 = -2\pi e^{\nu(y+y_o)}\cos\left[\nu(x-x_o)\right]
\end{aligned}$$

Motion derived as sum of singularities of the described kind automatically satisfy both kinematic and dynamic linearized conditions so that algorithms may be utilized, which are qualitatively similar to those developed for the potential flow of fully submerged bodies. In practice, formulations for simple singularities are substituted by expressions (8). More details on this subject are given by Wehausen and Laitone [4].

# 3 Method description

## 3.1 Problem statement

The flow field is modelled herein by a distribution of singularities (dipoles, vortices) determined by application of the boundary conditions on the body. Figure 1 shows a definition sketch for the problem. The fluid domain is bounded by the free surface, the foil surface and the bottom of infinite depth, while each streamline extends from $x = -\infty$ to $x = \infty$. The Cartesian coordinate system $(x$–$y)$ is right–handed and rectangular, with its origin taken at the intersection of the free surface level with the vertical line passing through the center of the foil chord. The $y$–axis points upwards, whereas the $x$–axis coincides with the undisturbed free surface. The hydrofoil experiences an incoming uniform stream of speed $V_o$ along the negative $x$–direction.

The following physical parameters are introduced: $c$, $t$, and $f$ denote the chord, thickness and camber of the hydrofoil section, respectively; $d$ is the submergence of the foil measured from the undisturbed free surface to the mid-chord; $\alpha$ is the angle of incidence; $\Gamma$ is the vortex strength; and $h$ is the crest–to–trough wave elevation at downstream. All variables have been normalized with respect to $c$, $V_o$ and $\rho$, being the latter the mass density of the fluid.

The problem is fully identified by the following variables: the depth-based Froude number, $Fn_d = V_o/\sqrt{gd}$, the ratio between the submergence and chord of the foil, $\eta = d/c$, and $\alpha$.

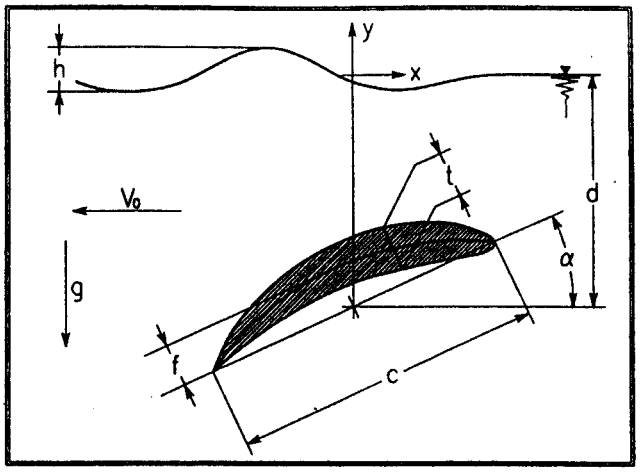

Figure 1: Computational domain

After the stream function is obtained, the nondimensional flow characteristics of a shallowly submerged hydrofoil may be computed as

- lift coefficient $C_L = 2\Gamma/(V_o \cdot c)$
- wave drag coefficient due to the generated waves $C_D = (h/c)^2/(8Fn_d^2 \cdot \eta)$
- pressure coefficient $C_P = 1 - (V/V_o)^2 - 2gy/V_o^2$

where $V$ is the obtained velocity at each considered point of the fluid domain.

## 3.2 Outline of the method

The submerged hydrofoil is represented by a distribution of dipoles and a vortex along the camber line. The field velocity is expressed as a gradient of a scalar velocity potential, governed by Laplace's equation in the fluid domain and subject to the aforesaid boundary conditions. An integral equation is thus derived, then reduced to a system of linear equations whose unknowns are the strength of the singularities.

A pair of dipoles are positioned at each singularity point, where the former is oriented horizontally and the latter vertically so that their linear combination yields a dipole oriented in proper direction. The first pair of dipoles is located at the center of the circle enveloping the hydrofoil surface at the leading edge; the second one rearward at a distance which is the product of the radius of the former circle with a constant $s_1$; all the remaining dipoles are positioned from each other at a distance $d = 0.5(t_1+t_2)/s_2$ where $t_1$ and $t_2$ are the hydrofoil thickness at the centres of neighbouring dipoles, respectively. In order to improve the convergence of the method, proper values have been simultaneously assigned to $s_1$ and $s_2$. After some convergence tests the constant values have been taken as $s_1 = 1.5165$ and $s_2 = 3.0$. In addition to the dipole distribution on the foil's camber line, a point vortex of strength $\Gamma$ is located at the center of the camber line which generates a circulatory flow superimposed onto the uniform incoming flow. An effective algorithm has been designed to distribute the dipoles of the basis flow at best. Numerical experiments have shown that values of $s_1$ and $s_2$ do not depend on the variation of the angle of incidence.

The arrangement of the dipole singularities along the camber line of the foil–stream system is shown in Figure 2, where the rear part of the hydrofoil around the trailing edge is represented magnified by a factor 17.5 with respect to the leading edge zone. Beyond virtually different representation, the streamlines are the same for both the zones.

Equations for the first pair of dipoles are written taking as control point the leading edge and imposing that the velocity is perpendicular to the normal of the body there while, at the same time, the stream function takes the same value it has at the trailing edge. In order to avoid undesirable fluctuations induced by the geometrical discontinuity, the control point simulating the trailing edge is located at a distance from it equal to half of the foil thickness there [2]. Distribution of the other control points are obtained by intersection of the profile with lines normal to the chord, going through the center of the corresponding singularities. Equations are derived by imposing that the stream function at the trailing edge has the same value at the control points, thus obtaining the required flow on the foil.

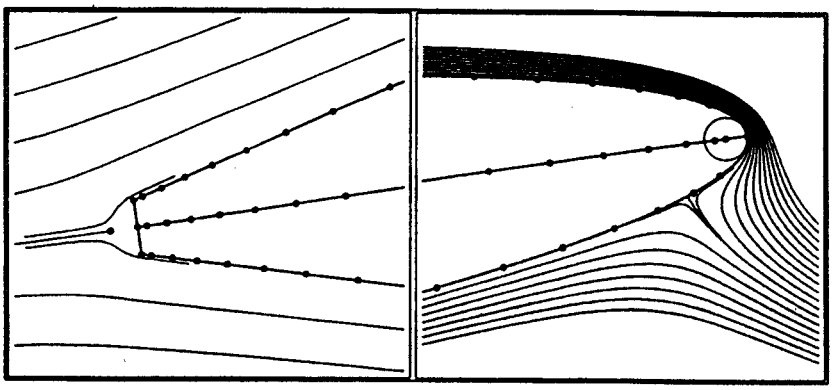

Figure 2: Representation of singularity distribution, control points and streamlines

The lift is introduced into the potential flow by applying the condition of finite velocity parallel to the tangent to the camber line at the trailing edge, e.g. the Kutta condition.

### 3.3 Computational aspects

In equations (8) for the two-dimensional singularities with linearized free surface, the third equation is an integral whose solution cannot be expressed in a simple algebraic form, so that it is considered in the Cauchy principal-value sense. This integral may be algebraically manipulated in a way resulting from the combination of the following terms

$$\int_{-a}^{\infty} \frac{e^x}{x} \cos(bx)dx \quad ; \qquad \int_{-a}^{\infty} \frac{e^x}{x} \sin(bx)dx \tag{9}$$

plus a simple algebraic expression. In this way, expressions similar to the third equation (8) are reduced in number of two simpler forms, namely equations (9). To solve these integrals an updated Simpson's method for approximate integration has been developed, whose behaviour shows to be very suitable for these functions (see Appendix).

## 4 Numerical results and discussion

The potential flow is determined from the solution (8) of the boundary value problem which has been formulated and discretized in the preceding sections. The presented numerical method has been used to compute the flow field around a NACA 16-012 wing section moving with constant speed under the free surface at different depth-based Froude numbers. Subsequently, the pressure field has been readily obtained from Bernoulli's equation. The values of wave drag, lift and pressure coefficients, have been derived in terms of $Fn_d$, $\eta$ and $\alpha$.

In order to evaluate applicability of linearization for the free–surface boundary condition in the case of the shallowly submerged hydrofoil, the wave elevations obtained by applying the kinematic boundary condition ($\psi$ = const.), the dynamic boundary condition ($C_P$ = const.) and the linearized relation given by $y = uV_0/g$, respectively, are shown in Figure 3. Since they have resulted slightly different, it has been deemed necessary to perform a numerical analysis of inaccuracies.

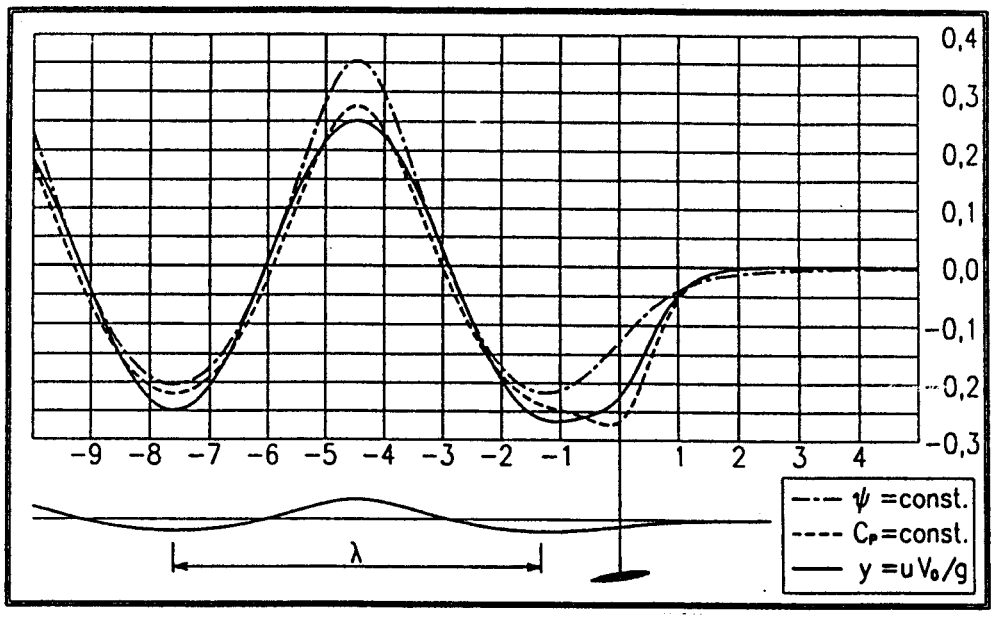


Figure 3: Wave elevations at various boundary conditions ($\eta = 1, Fn_d = 1, \alpha = 0.15$ rad)

To this purpose, the free–surface profile is assumed as the streamline produced by applying the boundary condition $\psi = 0$, since it is representative of the computed flow field. If the free–surface boundary condition were exact, the resulting pressure coefficient $C_P$ would be zero. Therefore, the maximum $C_P^*$ value evaluated at $x = 0$, may be assumed as a meaningful parameter to judge qualitatively and/or quantitatively the computed hydrodynamic results. Figure 4 illustrates the computed values of $C_P^*$ at different angles of incidence. The case $\alpha = 0$ may be considered as typical for angles of incidence within practical range of applicability, since the non–dependence of $C_P^*$ on $Fn_d$ allows to arrive at a simple and exhaustive diagram suitable to design purposes (Fig. 5). The value of maximum pressure on the free surface is represented in terms of submergence depth–to–chord ratio and speed given in knots. The designer should evaluate heuristically the allowable pressure threshold suitable for decision making at different design stages. On principle, higher values of pressure are allowable at higher speeds.

The final set of diagrams illustrated in the following is intended to provide exhaustive information on lift and drag at different values of $Fn_d$, $\eta$ and $\alpha$. They may be stored in a data base available to the designer for decision making. Although they are only a part of the global information stored in a data base, they give clear information on the hydrodynamic characteristics of the analysed hydrofoil. An overview of Figures 6 and 7 clearly confirms that both lift and drag present a jump around $Fn_d = 1$, which can be then considered as a critical velocity value. Figures 8 and 9 show how the influence of the free surface comes down to very little at increasing depth of submergence. Notice again that the foil drag is here the contribution due to wave–making only. When moving from 2–D to 3–D modelling in a real design situation, the system of divergent waves should

be reintroduced thus increasing the quasi–zero values of $C_D$.

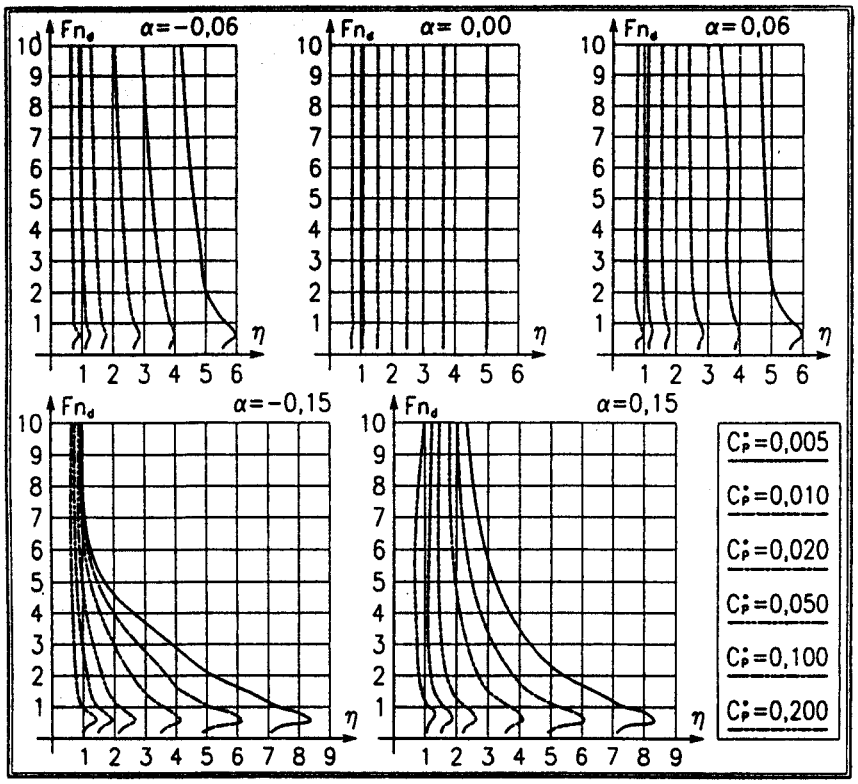


Figure 4: Maximum pressure coefficient on the free surface

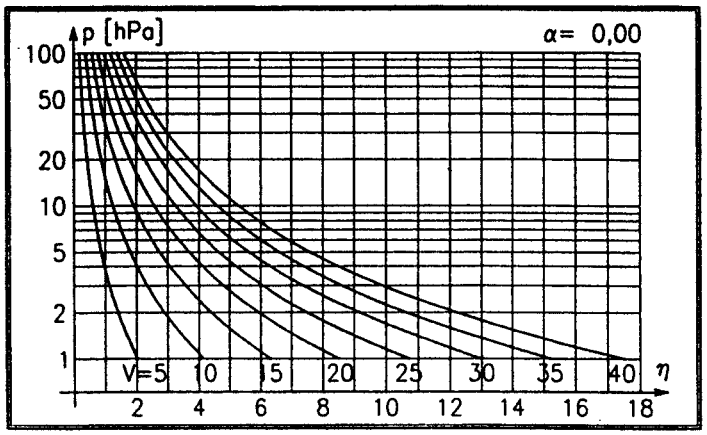


Figure 5: Feasibility abacus for marine vehicles

# 5 Concluding remarks

A simple but efficient numerical method has been developed to calculate the ideal, steady, incompressible, two–dimensional flow past a submerged hydrofoil. It is versatile in that arbitrary two–dimensional streamlined foils can also be handled. The proposed scheme uses a linear distribution of dipoles and vortex singularities on the foil's camber line. It has been shown that useful design results can be obtained, by which it is possible to evaluate how the free–surface waves affect the main hydrodynamic characteristics at shallow

submergence. This paper has tried to discuss some questions related to the accuracy and limits of applicability of free–surface boundary linearization too. Achieved results are accurate enough at medium speeds of current fast marine vehicles and submergence–to–chord ratio equal to 2 at least. Accordingly, operative situations which may be critical such as take–off of hydrofoil vessels can be studied by the proposed linearized method. In case of higher speeds and/or lower submergence depth only qualitative indications can be achieved which are however suitable and reliable to rank alternative design solutions.

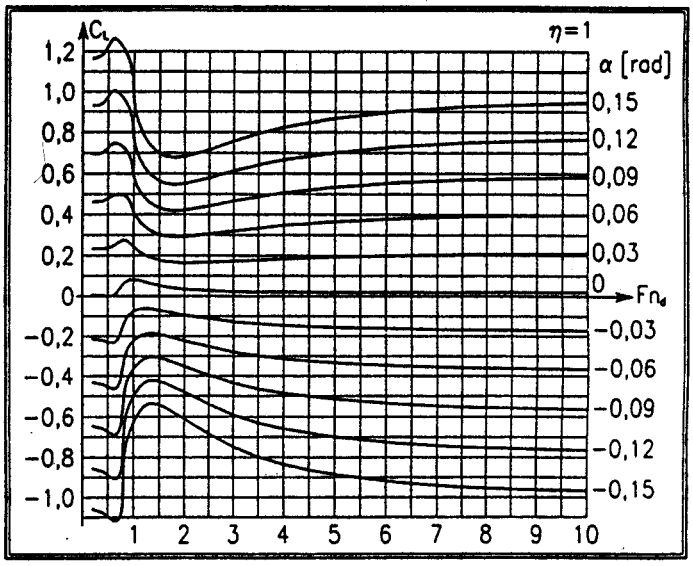


Figure 6: Lift coefficient versus depth–based Froude number

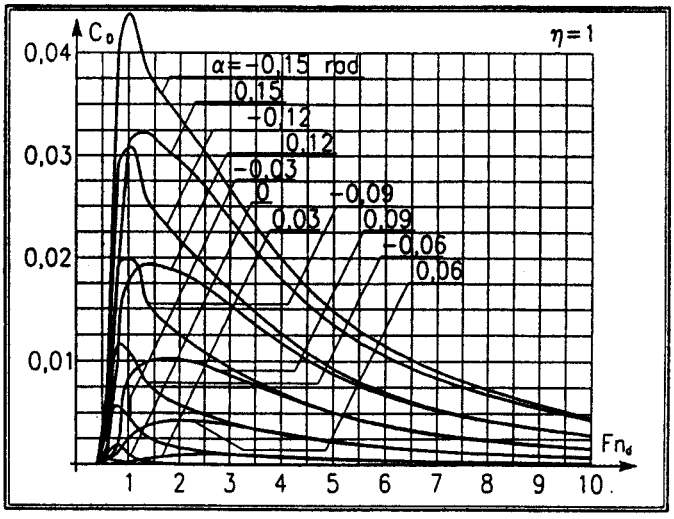


Figure 7: Drag coefficient versus depth–based Froude number

# References


[1] de'Vidovich, B., Trincas, G.: Numerical Method for the Calculation of Steady Linear Surface–Flow Past Submerged Hydrofoils, *Proceedings of NAV'97*, Napoli, 1997.

[2] Mattioli, E. : *Aerodinamica* (in Italian), Levrotto & Bella, Torino, 1980.

[3] Kočin, N.E., Kibel, I.A. and Roze, N.V.: *Theoretical Hydromechanics*, Moscow, Fifth Edition, Vol. 1, 1955, English Edition by Interscience Publishers, 1964.

[4] Wehausen, J.V. and Laitone, E.V.: *Surface Waves*, Handbuch der Physik, Springer-Verlag, Berlin, Band IX, pp. 461–490, 1960.

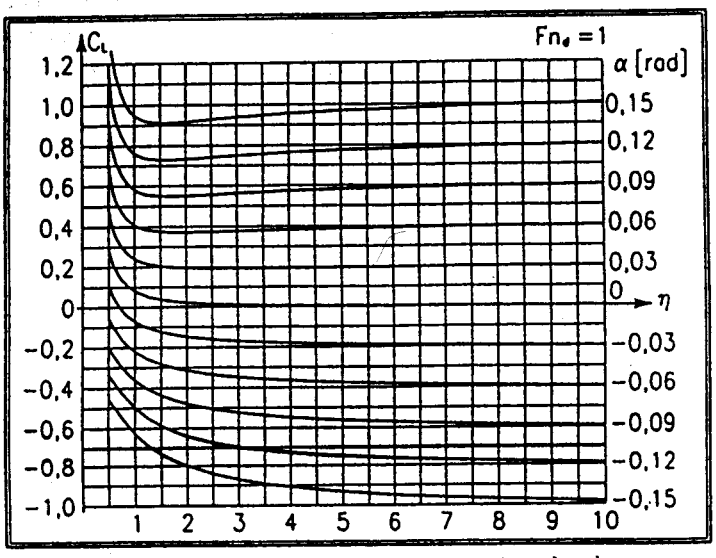


Figure 8: Lift coefficient versus nondimensional submergence

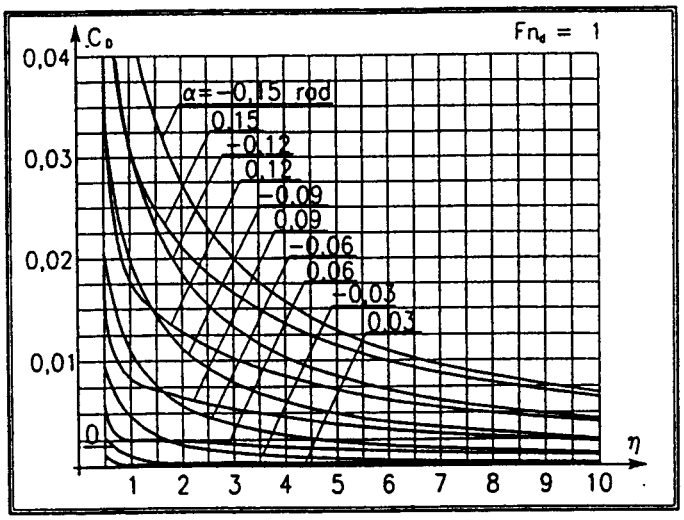


Figure 9: Drag coefficient versus nondimensional submergence

## Appendix

To determine the principal value of $I = \int_{x_1}^{x_3} \frac{f(x)}{x} dx$, the function $f(x)$ is substituted by a parabola, yielding

$$I = d + l(y_2 - 0.5d\xi)$$

in which

$$d = y_3 - y_1 - \xi(y_1 - 2y_2 + y_3) \; ; \quad y_1 = f(x_1) \; ; \quad y_2 = f(x_2) \; ; \quad y_3 = f(x_3)$$

$$x_2 = \frac{x_1 + x_3}{2} \quad ; \; \lambda = \frac{x_1 - x_3}{2} \quad ; \; \xi = \frac{x_2}{\lambda} \quad ; \; l = \ln \mid \xi + 1 \mid - \ln \mid \xi - 1 \mid$$

*La presente versione elettronica (.PDF)*
*è corrisponde a quanto presentato in occasione del*
*EIGHTH INTERNATIONAL CONFERENCE*
*ON COMPUTATIONAL METHODS AND EXPERIMENTAL MEASUREMENTS*
*Rodi 1997*

*Terminata l'undici febbraio MMI*